

6-4-2013

A Spectroscopic Analysis of the Eclipsing Short-Period Binary V505 Persei and the Origin of the Lithium Dip

Patrick Baugh
Clemson University

Jeremy R. King
Clemson University, jking2@clemson.edu

Constantine P. Deliyannis
Indiana University

Ann Merchant Boesgaard
University of Hawaii

Follow this and additional works at: https://tigerprints.clemson.edu/physastro_pubs

 Part of the [Astrophysics and Astronomy Commons](#)

Recommended Citation

Please use publisher's recommended citation.

This Article is brought to you for free and open access by the Physics and Astronomy at TigerPrints. It has been accepted for inclusion in Publications by an authorized administrator of TigerPrints. For more information, please contact kokeefe@clemson.edu.

A Spectroscopic Analysis of the Eclipsing Short-Period Binary V505 Persei and the Origin of the Lithium Dip

Patrick Baugh¹, Jeremy R. King¹, Constantine P. Deliyannis^{2,4}, and Ann Merchant Boesgaard^{3,4}

ABSTRACT

As a test of rotationally-induced mixing causing the well-known Li dip in older mid-F dwarfs in the local Galactic disk, we utilize high-resolution and -S/N Keck/HIRES spectroscopy to measure the Li abundance in the components of the ~ 1 Gyr, $[\text{Fe}/\text{H}] = -0.15$ eclipsing short-period binary V505 Per. We find $A(\text{Li}) \sim 2.7 \pm 0.1$ and 2.4 ± 0.2 in the $T_{\text{eff}} \sim 6500$ and 6450K primary and secondary components, respectively. Previous T_{eff} determinations and uncertainties suggest that each component is located in the midst of the Li dip. If so, their $A(\text{Li})$ are ≥ 2 – 5 times larger than $A(\text{Li})$ detections and upper limits observed in the similar metallicity and intermediate-age open clusters NGC 752 and 3680, as well as the more metal-rich and younger Hyades and Praesepe. These differences are even larger if the consistent estimates of the scaling of initial Li with metallicity inferred from nearby disk stars, open clusters, and recent Galactic chemical evolution models are correct. Our results suggest, independently of complementary evidence based on Li/Be ratios, Be/B ratios, and Li in subgiants evolving out of the Li dip, that main-sequence angular momentum evolution is the origin of the Li dip. Specifically, our stars' $A(\text{Li})$ indicates tidal synchronization can be sufficiently efficient and occur early enough in short-period binary mid-F stars to

¹Department of Physics and Astronomy, 118 Kinard Lab, Clemson University, Clemson, SC 29634-0978; pbaugh@clemson.edu, jking2@clemson.edu

²Department of Astronomy, Indiana University, Swain Hall West 319, 727 East 3rd Street, Bloomington, IN 47405-7105 USA; con@astro.indiana.edu

³Institute for Astronomy, University of Hawaii at Manoa, 2680 Woodlawn Drive, Honolulu, HI 96822, USA; boes@ifa.hawaii.edu

⁴Visiting Astronomer, W.M KECK Observatory, which is operated as a scientific partnership among the California Institute of Technology, the University of California and the National Aeronautics and Space Administration. The Observatory was made possible by the generous financial support of the W.M. Keck Foundation.

reduce the effects of rotationally-induced mixing and destruction of Li occurring during the main-sequence in otherwise similar stars that are not short-period tidally-locked binaries.

Subject headings: Stars – Star Clusters and Associations

1. INTRODUCTION

Lithium is of fundamental astrophysical importance. This fragile light element is quickly destroyed in stars when exposed to $T \geq 2.5 \times 10^6$ K, making it useful in studying matter transport in stars and providing observational feedback on our understanding of stellar structure and evolution (for a review, see Pinsonneault 1997). In addition, stellar Li abundances have cosmological applications. Combining the $A(\text{Li})^1$ in old stars with a) accurate stellar evolution models to account for stellar destruction, and b) accurate chemical evolution models to account for Galactic production, should lead to the primordial $A(\text{Li})$, which provides constraints on Big Bang nucleosynthesis (Boesgaard & Steigman 1985) and an independent check on cosmological parameters determined by WMAP (Coc et al. 2004). However, the vulnerability of Li to destruction that makes it a good probe of stellar interiors also complicates the derivation of *initial* halo dwarf $A(\text{Li})$ —our best connection to the Big Bang $A(\text{Li})$.

The astrophysical usefulness of Li, therefore, strongly depends on having correct stellar models that accurately trace the *in situ* history of Li. Standard² stellar models (SSMs) suggest that, for stars of about $1.2M_{\odot}$, the observed surface $A(\text{Li})$ can go down only, a) during the early pre-main sequence (PMS) when some of the interior Li is actually destroyed, and b) during subgiant evolution as the deepening surface convection zone (SCZ) dilutes it. Standard theory predicts no surface Li depletion during the main sequence (MS). More specifically, since Li burns at relatively low temperatures, anytime the SCZ reaches deep enough into the star’s interior, visible Li depletion will occur at the surface. This occurs during the PMS phase and, for stars of around $1.2M_{\odot}$, the SCZ is not deep enough during the MS to carry Li into the interior regions where it can be burned appreciably. Even during late PMS convective burning, such depletion is minimal. For a $1.2M_{\odot}$ star with $[\text{Fe}/\text{H}] \leq -0.1$, the maximum expected depletion on both the MS and the PMS is < 0.1 dex (Pinsonneault

¹ $A(Li) \equiv \log N(Li)$ on the usual scale where the logarithmic number abundance of hydrogen is given by $\log N(H) \equiv 12$.

²That is, spherically symmetric models that ignore rotation, diffusion, mass loss, magnetic fields, and other physics that could affect real stars (Deliyannis, Demarque & Kawaler 1990; Pinsonneault 1997).

1997). Therefore, little Li depletion in stars of this mass (or higher) is expected on the PMS, and virtually none on the MS, based on the predictions from SSMS (Deliyannis 1998).

In contradistinction, striking Li (Boesgaard & King 2002, and Be;) depletion is observed in disk MS stars with $6300 \leq T_{\text{eff}} \leq 6900$ K. In the Hyades, Boesgaard & Tripicco (1986) discovered that stars with $6500 \leq T_{\text{eff}} \leq 6850$ K were depleted by $\geq 0.5 - 2$ dex as compared to stars merely 200–300 K hotter or cooler. This abrupt F-star Li(Be) depletion (the Li dip) occurs mainly *during the MS*, since much younger clusters such as the Pleiades (~ 100 Myr) show a nearly flat Li- T_{eff} relation (Boesgaard, Budge & Ramsay 1988; Soderblom et al. 1993). The Li dip presents a challenge to SSMS, which predict negligible Li depletion on the MS, and casts doubt on their ability to either predict or backtrack Li abundances to initial values. Instead, stellar models are required that can explain the Li dip accurately by modeling Li abundances over a star’s lifetime. A number of refinements to SSMS have been proposed to explain the Li dip (Balachandran 1995; Deliyannis 2000; Sestito & Randich 2005), but here we focus on rotationally-induced mixing (RIM) (Charbonnel & Vauclair 1992; Pinsonneault et al. 1992). RIM models propose that a loss of angular momentum, as stars spin down on the MS, could cause slow mixing between the photosphere and the hotter denser region beneath the SCZ, resulting in the depletion of surface Li.

To test this theory, Ryan & Deliyannis (1995) suggest that Li abundances of short-period tidally-locked binaries (SPTLBs) be measured. RIM and stellar tidal theory (Zahn & Bouchet 1989) together predict that a SPTLB loses most of its angular momentum during the very early PMS, when interior densities and temperatures are too low to burn Li. Hence, lacking significant angular momentum to lose and drive future requisite mixing, neither does it suffer MS Li depletion responsible for the Li dip. Thus, one method to test if angular momentum transfer is indeed the causal force behind the Li dip is to find SPTLBs whose ages and temperatures should place them in the Li dip, and measure their Li. A value of $A(\text{Li})$ higher than otherwise similar Li dip stars would support RIM models. V505 Persei, a Pop I intermediate-age short-period binary system, is made up of two F stars of nearly equal mass, radius, and T_{eff} (Marschall et al. 1997; Tomasella et al. 2008). Both masses, T_{eff} , and ~ 4 day period make them good candidates to test if an early PMS loss of angular momentum can later preserve Li compared to otherwise similar non-SPTLB stars. We measure the $A(\text{Li})$ s of V505 Per and compare them in the $A(\text{Li})$ versus zero-age MS (ZAMS) T_{eff} plane with stars of intermediate-age open clusters, showing in the process that the components of V505 Per have $A(\text{Li})$ s higher than single stars of their ZAMS T_{eff} .

2. DATA AND ANALYSIS

2.1. Observations

High-resolution ($R = 45,000$) spectroscopy of HD 14384 was obtained on 30 and 31 August 1997 using Keck/HIRES. Three nightly exposures totalled 8 and 5.5 minutes on the first and second nights, respectively. Debiasing, flat-fielding, scattered light removal, order tracing/extraction, and wavelength calibration were carried out with standard routines in IRAF.

Given the short integration spans relative to the 4.2 d period, we co-added the 3 nightly spectra. The resulting $\lambda 6707$ continuum level Poisson SNR/pixel is 850 and 580 on the first and second nights. Spectra were fit with a low order polynomial to perform a continuum normalization. Figure 1 shows our co-added, normalized spectra. The physically similar components of the SB2 are distinguished and identified both by slight differences in the strengths of the $\lambda 6717$ CaI feature and the relative Doppler shifts expected from the orbital ephemeris of Tomasella et al. (2008). The relative Doppler shifts of the components in each night’s coadded spectrum, needed for the spectrum synthesis described next, were measured from the centroids of the CaI features.

2.2. Syntheses and Comparison

To derive Li and Fe abundances, we conducted spectrum synthesis of the $\lambda 6707$ Li I region to account for the line blending between the stellar components. Such synthesis requires knowledge of T_{eff} , $\log g$, radius (R), and microturbulent velocity (ξ) of each star. The first of three of these parameters are taken from Tomasella et al. (2008), who determine radii and associated uncertainties from a Wilson & Devinney (1971) code-based solution with updated model stellar atmospheres (Milone, Stagg, & Kurucz 1992); these radii agree with alternate solutions derived from the radial velocities and BV photometry alone to within $0.05 R_{\odot}$, which is well within their stated $\pm 0.11 R_{\odot}$ uncertainty adopted here. The T_{eff} values and uncertainties of Tomasella et al. (2008), 6512 ± 21 and 6462 ± 12 K for the A and B components, are derived from multiparameter χ^2 fitting of 700 \AA of their own high-resolution ($R \sim 20,000$) spectra against synthetic spectra grids. Encouragingly, the T_{eff} differences of the components they derive as part of the orbital solutions agree to within 18 K of the spectroscopically-derived value.

The Tomasella et al. (2008) masses and radii yield $\log g = 4.33 \pm 0.02$ for both components. We determined ξ (1.73 and 1.70 km s^{-1}) using the T_{eff} - and $\log g$ -dependent calibration

of Allende Prieto et al. (2004). We note, though, the derived Li abundances are insensitive to the value of $\log g$ and ξ . While $[\text{Fe}/\text{H}]$ was eventually determined from a comparison of the observed and synthetic spectra, we adopted an initial metallicity of $[\text{Fe}/\text{H}] = -0.35$ from the photometric determination of Nordström et al. (2004).

We used the T_{eff} , $\log g$, and $[\text{Fe}/\text{H}]$ values to interpolate model atmospheres from the grids of Kurucz (1992). MOOG³ was used to create a synthetic spectrum for each star using the $\lambda 6707$ linelist of King et al. (1997). The spectra were smoothed by convolving with a Gaussian with FWHM measured from clean, weak lines in the observed spectra. Each component’s synthetic spectrum was Doppler shifted and then combined, using the product of the square radii and the Planck function value at 6707\AA (a pseudo-monochromatic luminosity) as a weighting factor. This correction for flux dilution is appropriate for the first night’s observations (orbital phase of 0.74) since each star’s undiminished flux contributes to the spectrum. The orbital phase (0.97) of second night’s observations places the system on the cusp of primary eclipse; however, the eclipses are very sharp, and the total system flux diminishment in B at this phase is $\lesssim 0.01$ mag of the ~ 0.5 mag total at primary eclipse.

Finally, we compared the synthetic spectra to the observed spectra using χ^2 minimization methods. We used the $\lambda 6705$ Fe I line to determine $[\text{Fe}/\text{H}]$, forcing both stars to have an assumed identical Fe abundance. Once a best-fit value of $[\text{Fe}/\text{H}]$ had been determined, we moved on to $A(\text{Li})$, which was allowed to differ in the two components to allow for possible differing Li depletion in the two stars. These synthetic spectra are compared to the observed data in Figure 1.

2.3. Results

The analysis of the first night’s data yielded $[\text{Fe}/\text{H}] = -0.15 \pm 0.03$. The quoted error is due to the 1σ level fitting uncertainties alone; even so, our metallicity estimate is in good agreement with $[\text{M}/\text{H}] = -0.12 \pm 0.03$ from Tomasella et al. (2008). The metallicity from the second night was not calculated due to the unfortunate placement of the $\lambda 6705$ FeI feature in the secondary star with a detector/reduction artifact that can be seen in Figure 1; in carrying out the Li syntheses, we assumed the $[\text{Fe}/\text{H}]$ value from the first night’s data.

The Li syntheses (Figure 1) yield average $A(\text{Li})$ of 2.67 ± 0.1 and 2.42 ± 0.2 for the primary and secondary components, respectively. While the best-fit Li abundances differ by only a few hundredths of a dex, the larger quoted uncertainties in $A(\text{Li})$ are dominated by

³<http://as.utexas.edu/chris/moog.html>

uncertainties in the continuum location. Contributions from fitting uncertainties in the χ^2 minimization and T_{eff} uncertainties amount to only $\pm 0.03 - 0.06$ dex and $\pm 0.01 - 0.02$ dex, respectively; contributions from uncertainties in ξ and $\log g$ are similarly small or smaller and are ignored. Abundance uncertainties arising from uncertainties in the flux dilution factors of each component, which in turn arise from uncertainties in T_{eff} and the Tomasella et al. (2008) stellar radii, are $0.01 - 0.02$ dex.

3. DISCUSSION

3.1. Li versus ZAMS T_{eff}

Interpreting the A(Li) of our SPTLB components requires that they be placed in the context of the Li dip morphology defined by other single (or non-SPTLB) stars. In her comparisons of the Li dip in various open clusters, Balachandran (1995) found that the T_{eff} at which the Li dip occurs varies based on metallicity, but that the ZAMS T_{eff} at which the Li dip is located does not; this provides a means by which the Li dip morphology of different populations of disk stars can be compared. Additionally, Balachandran (1995) found that the morphology of the cool side of the Li dip is age-dependent. Some evidence suggests that the Li dip may begin to form as early as an age of 150 Myr (Steinhauer & Deliyannis 2004) or even 100 Myr (Margheim 2007). Clearly, comparing our stars with bona fide Li dip stars requires knowledge of our SPTLB components' ZAMS T_{eff} and age.

For consistency, we followed the approach of Balachandran (1995) to find the ZAMS T_{eff} of each star by looking at differences implied by isochrones (and their assumed color transformations) between our stars in their current evolutionary state and on the ZAMS. This required that we first determine the age of our SPTLB stars, which we did by placing the components in the radius versus mass plane and comparing these locations with sequences from $[m/H] = -0.14$ Yonsei-Yale isochrones (Demarque et al. 2004). As shown in Figure 2, this implies an age of 1.15 ± 0.15 Gyr for the system; the majority of the age uncertainty comes from uncertainty in the radii estimates.

We then used the Yonsei-Yale isochrones with the Green color-temperature relations, which are also employed by the Revised Yale Isochrones (Green, Demarque, & King 1987) used by Balachandran (1995), to determine the difference between the T_{eff} at 1.15 Gyr and on the ZAMS. This T_{eff} difference was then applied to our current T_{eff} value from Tomasella et al. (2008), yielding ZAMS T_{eff} values of 6483 and 6432K for the primary and secondary components. The 1σ level uncertainties in our interpolation of the T_{eff} -mass relations of the isochrones are ≤ 12 K.

Figure 3 presents the Li-ZAMS T_{eff} diagram containing: the V505 Per components; the literature data reanalyzed by Balachandran (1995) for the open cluster NGC 752, having a 1.45 Gyr age (Anthony-Twarog et al. 2009) and $[\text{Fe}/\text{H}] = -0.15$ (Daniel et al. 1994); the Li data for the 1.75 Gyr, $[\text{Fe}/\text{H}] = -0.08$ cluster NGC 3680 (Anthony-Twarog et al. 2009); and the Li data of Balachandran (1995) for the 650 Myr $[\text{Fe}/\text{H}] = +0.13$ Hyades cluster. We determined the NGC 3680 object masses using a Legendre polynomial relation to map the dual V magnitude and mass abscissas of Figure 4 of Anthony-Twarog et al. (2009). We then used the Yonsei-Yale isochrones as described above to determine the T_{eff} difference between the ZAMS and at 1.75 Gyr at a given mass. This difference was then applied to the AT2009 T_{eff} values to yield ZAMS T_{eff} values.

3.2. v505 Per versus the Hyades

If the v505 Per T_{eff} values and uncertainties of Tomasella et al. (2008) are reliable, and if the *relative* uncertainties in the to-ZAMS T_{eff} corrections for the v505 Per components compared to those of the open cluster comparison stars are not several times the size of the corrections themselves (~ 30 K for our binary components and ~ 40 K for similar mass stars in the slightly older NGC 752 cluster), then Figure 3 indicates that both our SPTLB components are positioned inside the Li dip that is well defined by the Hyades data (or those of the Praesepe data not shown here; see Figure 12 of Balachandran 1995). The larger Li abundances in the v505 Per components compared to nearly all of the younger and more metal-rich Hyades data in Figure 3 is especially notable given the metallicity difference and the age difference, which we discuss in turn, between the two.

First, comparisons of the v505 Per Li abundances with those in cluster stars are most meaningful if some account of initial Li abundance differences can be made. An empirical approach to parameterize Galactic disk Li production in terms of Fe production is to use the upper envelope of the Li-Fe relation exhibited by large samples of field stars. The field star data over the range $-1 \leq [\text{Fe}/\text{H}] \leq 0$ in Figure 7 of Lambert, Heath & Edvardsson (1991) suggest an initial Li-to-Fe (logarithmic by number) relation in the local disk having slope ~ 1 dex/dex. For comparison, the Galactic chemical evolution model in Figure 9 of Travaglio et al. (2001) produces a slope of ~ 0.7 dex/dex over the same $[\text{Fe}/\text{H}]$ range, though this slope may be too small since it is unable to reproduce the initial solar Li abundance. Indeed, determinations of the slope of the Li-to-Fe relation using Li abundances on the G-dwarf Li peak of various open clusters are significantly larger at 1.4 dex/dex (Boesgaard 1991) and 1.0 dex/dex (Cummings 2011).

The Hyades and Praesepe have super-solar metallicities: $[\text{Fe}/\text{H}] \sim +0.10$ to $+0.15$

(Boesgaard 1989; Boesgaard & Friel 1990). The local disk field and Cummings (2011) open cluster Li-Fe relation thus implies the initial Hyades and Praesepe Li abundances were a factor of 2 larger than for the v505 Per components; the Boesgaard (1991) open cluster Li-Fe relation implies initial Li abundances a factor of 2.6 larger than for the v505 Per components. Accounting for initial Li differences in this way makes the observed present-day difference between v505 Per and Hyades Li abundances even more remarkable.

Second, the red side of the Li dip is known to flatten with increasing age, which may be due to increasing Li depletion in the dip stars with age (Balachandran 1995). Nevertheless, despite their older age, our SPTLB components exhibit Li abundances a factor of 2 *larger* than nearly all Li detections or upper limits at similar ZAMS T_{eff} in the younger (~ 650 Myr) Hyades and Praesepe. Once reaching the v505 Per age, stars on the red side of the dip in these clusters would presumably have even lower Li abundance than at present.

3.3. Comparison with other data

Figure 3 also compares V505 Per with stars of more similar $[\text{Fe}/\text{H}]$: those in NGC 752 and NGC 3680. The $A(\text{Li})$ of our SPTLB components are a factor of 2-5 larger than the upper limits for the NGC 752 and NGC 3680 Li dip stars (one 3680 star on the steep blue side of the dip is within the error bar of our primary component). Note that Sestito, Randich & Pallavicini (1994) argue that their high-resolution spectroscopy of solar-type dwarfs in NGC 752 suggests $[\text{Fe}/\text{H}] = +0.01$ for this cluster, 0.15 dex larger than the canonical value quoted by Daniel et al. (1994). If so, the above discussion of the initial Li abundance versus $[\text{Fe}/\text{H}]$ relation suggests an even larger difference between the Li depletion factors of our SPTLB components and the NGC 752 Li dip stars.

Finally, it is important to recall that the preservation of Li by SPTLBs occurs if angular momentum loss occurs sufficiently early during the PMS, when interior temperatures and densities are too low to burn Li. This early synchronization is predicted to occur in systems with periods below some critical period that is a function of stellar mass and metallicity (Zahn 1994). The models of Zahn (1994) for Galactic disk stars of mass $1.2M_{\odot}$ indicate this critical period is 6 days. The 4.2d period of V505 Per falls under this critical period, though the 1.25 and $1.27M_{\odot}$ components slightly exceed the $1.2M_{\odot}$ maximum mass considered by the modeling of Zahn (1994). The Hyades SPTLB vB 34 resides within the blue region of the Hyades Li gap, but does not clearly demonstrate a Li abundance larger than similar single stars (see, e.g., Figure 1 of Ryan & Deliyannis 1995). However, Yonsei-Yale isochrones ($[\text{Fe}/\text{H}] = +0.13$, 650 Myr for the Hyades; $[\text{Fe}/\text{H}] = -0.14$, 1.15Gyr for v505 Per) indicate that the vB 34 masses are $0.20\text{-}0.23M_{\odot}$ larger than for v505 Per; thus, the 3.1d period of vB

34 may not be below a necessary critical period for its larger mass components.

4. CONCLUSIONS

Lithium is important for probing stellar interiors and evolution. It can be used to study transport of matter in the stars, Galactic chemical evolution, and BBN. Such uses depend heavily on accurate predictions of Li abundance evolution within stars. It is known that SSMs are unable to explain the Li dip in disk mid-F dwarfs. Modified stellar models that include the action of rotationally-induced slow mixing can explain the Li dip as the result of slow Li mixing in stars that are currently undergoing angular momentum loss and are sufficiently massive that interior temperatures and densities are sufficiently large to burn Li as a result of such mixing.

Although other types of physical mechanisms have also been proposed as explanations of the Li dip, including diffusion, mass loss, and other types of mixing, a variety of observational evidence favors, often quite strongly, the RIM-type models over other mechanisms. This evidence includes (but is not limited to): a) the Li/Be depletion correlation where *both* elements are depleted, but Li more severely (Stephens et al. 1997; Deliyannis et al. 1998; Boesgaard et al. 2004) b) the Be/B depletion correlation (Boesgaard, Deliyannis & Steinhauer 2005) c) subgiants in M67 revealing the size and shape of the (MS) stellar preservation region as they evolve out of the cool side of the Li dip (Sills & Deliyannis 2000) d) and the early MS formation of the Li dip.

Here, we present an independent observational test of the RIM explanation of the Li dip. The T_{eff} values and uncertainties of Tomasella et al. (2008) indicate that the components of the mildly metal-poor ($[\text{Fe}/\text{H}] \sim -0.15$) intermediate-age ($\sim 1.1\text{Gyr}$) short-period tidally-locked binary V505 Per both reside in the Pop I Li dip defined by open cluster observations (assuming the differential $\sim 10\text{ K}$ to-ZAMS T_{eff} corrections suggested by isochrones for our stars relative to the younger Hyades and older NGC 752 and NGC 3680 clusters are not, in fact, an order of magnitude larger). If angular momentum loss in such a system occurred very early during the pre-main sequence phase, then it would suffer no or reduced RIM during the MS compared to non-SPTLB stars occupying the Li dip region; as a result, the V505 Per components would exhibit larger Li abundances than otherwise similar stars in the Li gap.

We find that the V505 Per components' Li abundances are at least 2-5 times larger than both: a) the Li upper limits in the $\sim 1.5\text{--}2\text{Gyr}$ and similarly mildly metal-poor ($[\text{Fe}/\text{H}] \sim -0.15$ and -0.08) clusters NGC 752 and 3680, and b) the upper limits and Li detections in the

younger metal-rich Hyades and Praesepe clusters. If there exists an initial Li-Fe relation of positive slope, as field star data and open cluster observations and Galactic chemical evolution models each independently suggest, and initial Li abundances indeed scale with $[\text{Fe}/\text{H}]$ in the recent disk, then the Li overabundance of V505 Per is even more dramatic in the case of the younger clusters (which presumably started with a higher initial Li abundance) and perhaps in NGC 752 if one assumes the higher $[\text{Fe}/\text{H}]$ value of Sestito, Randich & Pallavicini (1994).

Our results suggest, independently, that angular momentum evolution on the MS is responsible for the Li dip, confirming the conclusions drawn from the variety of observational evidence listed above, involving both field and cluster dwarfs. SPTLBs with higher-than-normal Li have been found in the 650-Myr old Hyades (Thorburn et al. 1993, see Soderblom et al. 1990 for a related idea), the 4.5Gyr-old M67 (Deliyannis et al. 1994), and in other contexts (Ryan & Deliyannis 1995); and, significantly, SPTLBs have *normal* Li in clusters, such as the Pleiades, which are too young for much RIM-related depletion to have occurred (Ryan & Deliyannis 1995). Our results for V505 Per complement these previous findings in that the V505 Per SPTLB stars are the hottest high-Li SPTLBs discovered so far, and are indeed very close to the limiting T_{eff} beyond which the models of Zahn (1994) can no longer synchronize both components sufficiently early during the pre-MS to prevent Li destruction. The SCZ of hotter SPTLBs is too shallow and their Hayashi paths too short for the components to grab onto each other sufficiently effectively so as to cause tidal locking during that same evolutionary phase.

While the Li abundances in our V505 Per components likely reflect some Li depletion from a plausible initial abundance in the range $A(\text{Li}) = 3.0 - 3.3$, which is not unexpected (see section 2.2.1 of Ryan & Deliyannis 1995), they nevertheless suggest that early tidal circularization can be efficient in mid-F stars in the Li dip and mitigate the effects of RIM on Li depletion. Identification of additional Li dip SPTLBs, analysis of their $A(\text{Li})$, and comparison with that of single stars of similar Li dip position, metallicity, and age would be a profitable means to extend these conclusions.

This work was supported by NSF awards AST-0239518 and AST-0908342 to JRK, and AST-0607567 to CPD. We thank Bruce Twarog for providing us with the NGC 3680 data.

Facility: KECK

REFERENCES

- Allende Prieto, C., Barklem, P. S., Lambert, D. L., & Cunha, K., 2004, *A&A*, 420, 183
- Anthony-Twarog, B. J., Deliyannis, C. P., Twarog, B. A., Croxall, K. V., & Cummings, J. D. 2009, *AJ*, 138, 1171
- Balachandran, S., 1995, *ApJ*, 446, 203
- Boesgaard, A. M., & Steigman, G., 1985, *ARA&A*, 23, 319
- Boesgaard, A. M., & Tripicco, M., 1986, *ApJ*, 302, L49
- Boesgaard, A.M., Budge, K. G. & Ramsay, M. E. 1988, *ApJ*, 327, 389
- Boesgaard, A. M. 1989, *ApJ*, 336, 798
- Boesgaard, A. M., & Friel, E. D. 1990, *ApJ*, 351, 467
- Boesgaard, A. M. 1991, *ApJ*, 370, L95
- Boesgaard, A. M., & King, J. R. 2002, *ApJ*, 565, 587
- Boesgaard, A. M., Armengaud, E., King, J. R., Deliyannis, C. P., & Stephens, A., 2004, *ApJ*, 613, 1202
- Boesgaard, A. M., Deliyannis, C. P., & Steinhauer, A. S. 2005, *ApJ*, 621, 991
- Cayrel de Strobel, G., 1990, *Mem. Soc. Astron. Italiana*, 61, 613
- Charbonnel, C. & Vauclair, S, 1992, *A&A*, 265, 191
- Coc, A., Vangioni-Flam, E., Descouvemont, P., Adahchour, A., & Angulo, C., 2004, *ApJ*, 600, 544
- Cummings, J. 2011, PhD dissertation, Indiana University
- Daniel, S. A., Latham, D. W., Mathieu, R. D., & Twarog, B. A., 1994, *PASP*, 106, 281
- Deliyannis, C. P., Demarque, P., & Kawaler, S. D. 1990, *ApJS*, 73, 21
- Deliyannis, C. P., King, J. R., Boesgaard, A. M., & Ryan, S. G. 1994, *ApJ*, 434, L71
- Deliyannis, C. P., Boesgaard, A. M., Stephens, A., King, J. R., Vogt, S. S., & Keane, M. J. 1998, *ApJ*, 498, L147

- Deliyannis, C. P. 2000, ASPCS, 198, 238
- Deliyannis, C., 1998, in *Workshop on Subaru HDS: Decipherment of Cosmic History with Spectroscopy*, eds. M. Takeda-Hidai & H. Ando, (Hilo, HI, USA: National Astronomical Observatory of Japan) p. 115
- Demarque, P., Woo, J.-H., Kim, Y.-C., & Yi, S. K., 2004, ApJS, 155, 667
- Green, E. M., Demarque, P., & King, C. R., 1987, *The Revised Yale Isochrones and Luminosity Functions* (New Haven: Yale Univ. Obs.)
- King, J. R., Deliyannis, C. P., Hiltgren, D. D., Stephens, A., Cunha, K., & Boesgaard, A. M., 1997, AJ, 113, 1871
- Kurucz, R. L., 1992, Rev. Mexicana Astron. Astrofis., 23, 181
- Lambert, D. L., Heath, J. E., & Edvardsson, B. 1991, MNRAS, 253, 610
- Margheim, S. J. 2007, PhD Dissertation, Indiana University
- Marschall, L., Stefanik, R., Lacy, C., Torres, G., Williams, D., & Agerer, F., 1997, AJ, 114, 793
- Milone, E. F., Stagg, C. R., Kurucz, R. L. 1992, ApJS, 79, 123
- Nordström, B., Mayor, M., Andersen, J., Holmberg, F., Pont, F., Jørgensen, B. R., Olsen, E. H., Udry, S., & Mowlavi, N., 2004, A&A, 418, 989
- Pinsonneault, M., 1997, ARA&A, 35, 557
- Pinsonneault, M. H., Deliyannis, C. P., Demarque, P., 1992, ApJS, 78, 179
- Ryan, S., Deliyannis, C., 1995, ApJ, 453, 819
- Sestito, P., Randich, S., & Pallavicini, R., 1994, A&A, 426, 809
- Sestito, P., & Randich, S. 2005, A&A, 442, 615
- Sills, A. I., & Deliyannis, C. P. 2000, ApJ, 544, 944
- Soderblom, D. R., Oey, M. S., Johnson, D. R. H., & Stone, R. P. S. 1990, AJ, 99, 595
- Soderblom, D. R., Jones, B. F., Balachandran, S., Stauffer, J. R., Duncan, D. K., Fedele, S. B., & Hudon, J. D. 1993, AJ, 106, 1059

- Steinhauer, A., & Deliyannis, C. P. 2004, *ApJ*, 614, L65
- Stephens, A., Boesgaard, A. M., King, J. R., & Deliyannis, C. P., 1997, *ApJ*, 491, 339
- Thorburn, J. A., Hobbs, L. M., Deliyannis, C. P., & Pinsonneault, M. H. 1993, *ApJ*, 415, 150
- Tomasella, L., Munaris, U., Siviero, A., Cassisi, S., Dallaporta, S., Zwitter, T., & Sordo, R., 2008, *A&A*, 480, 465
- Travaglio, C., Randich, S., Galli, D., Lattanzio, J., Elliott, L. M., Forestini, M., & Ferrini, F., 2001, *ApJ*, 559, 909
- Wilson, R. E., & Devinney, E. J. 1971, *ApJ*, 166, 605
- Zahn, J.-P., & Bouchet, L., 1989, *A&A*, 223, 112
- Zahn, J.-P. 1994, 1994, *A&A*, 288, 829

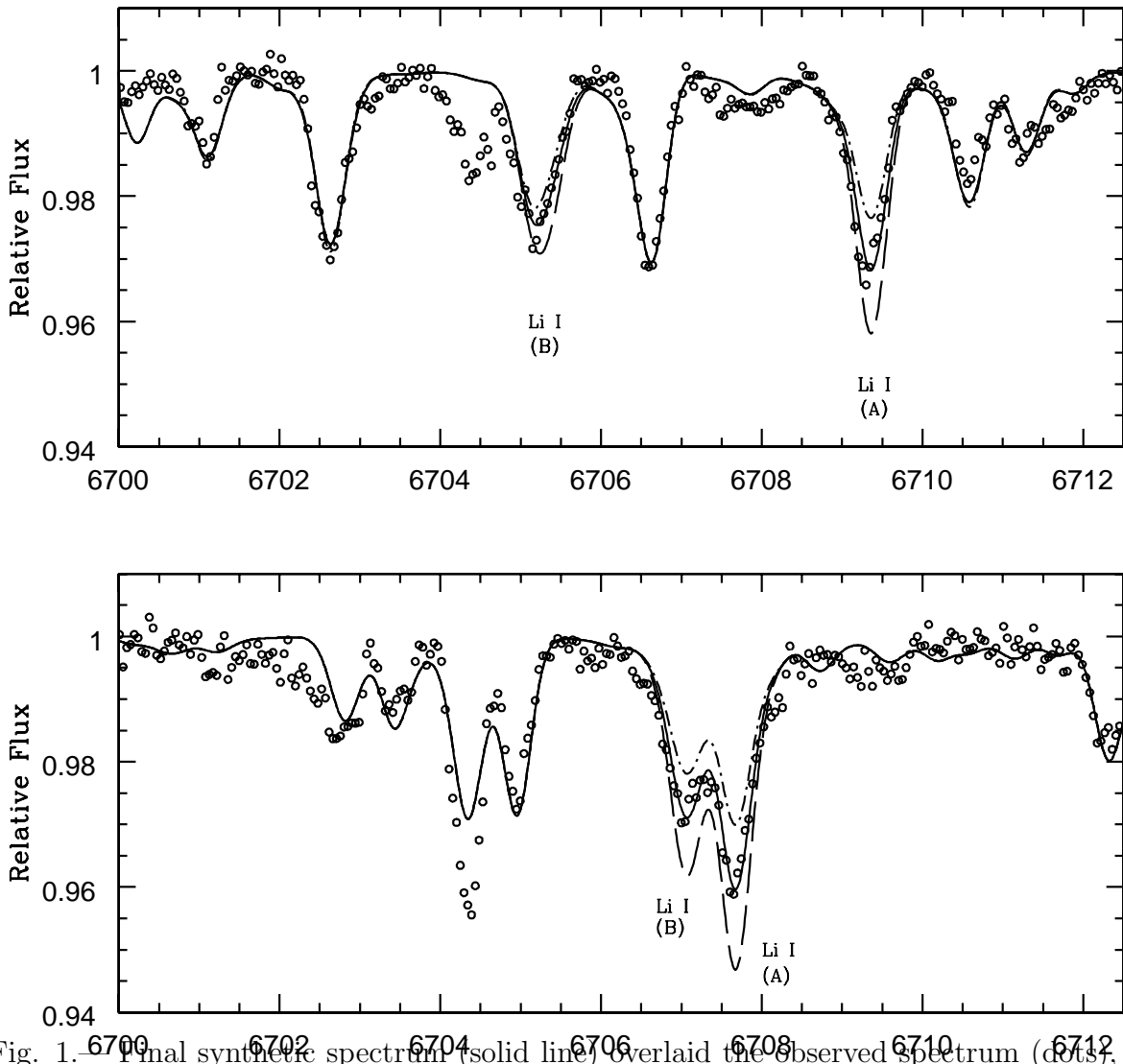


Fig. 1.— Final synthetic spectrum (solid line) overlaid the observed spectrum (dots), with two other synthetic spectra offset in Li abundance by ± 0.15 dex for comparison (dashed and dotted lines). The top and bottom panels show the coadded spectra for 30 Aug and 31 Aug, respectively. The “feature” at 6704.5Å is an artifact that contaminates the Fe I line of the B component in the second night’s spectrum.

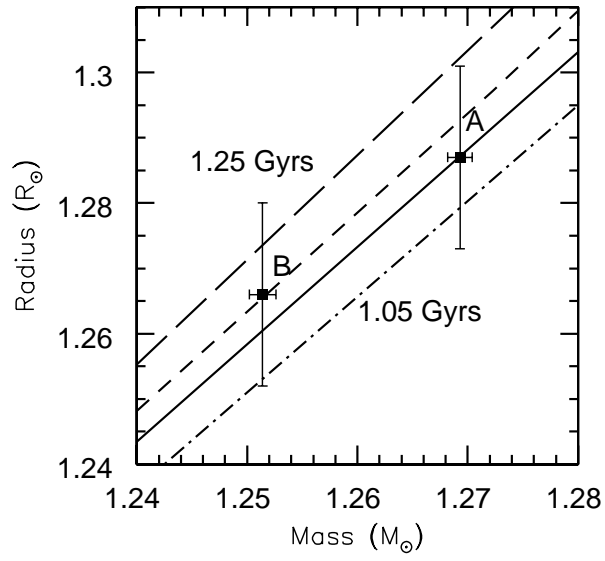


Fig. 2.— Yonsei-Yale isochrones (lines) for $[\text{Fe}/\text{H}] = -0.14$ and $[\alpha/\text{Fe}] = 0$ from 1.05-1.25 Gyr plotted in the radius versus mass plane with the physical determinations of the V505 Per A and B components.

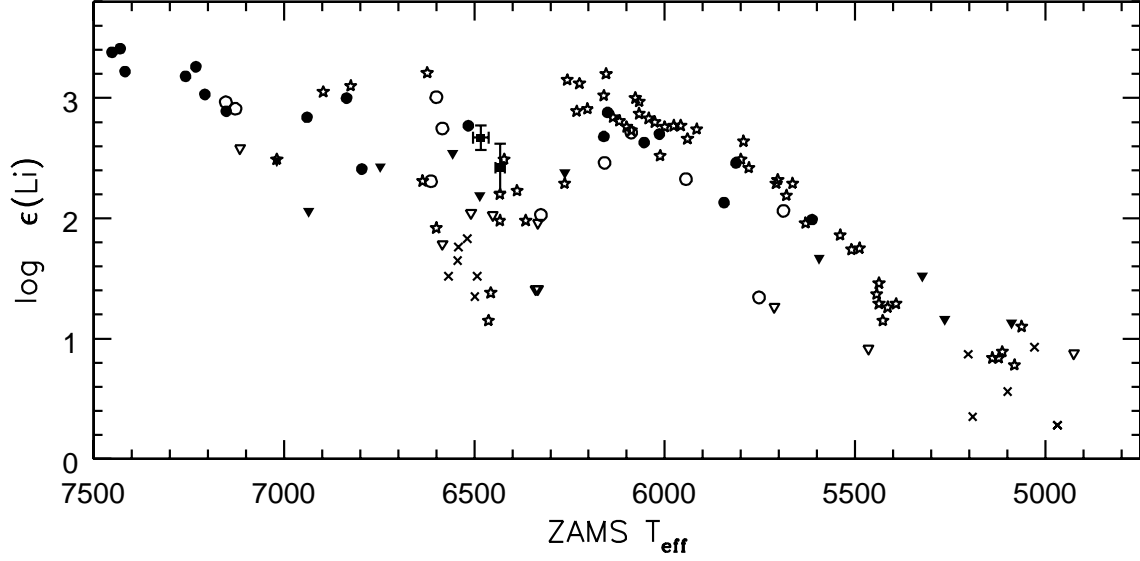


Fig. 3.— $A(\text{Li})$ versus ZAMS T_{eff} plane containing: the V505 Per components (solid squares); objects in the 1.45Gyr-old (Anthony-Twarog et al. 2009) cluster NGC 752 (open circles; inverted open triangles are upper limits) taken from the reanalysis of Balachandran (1995); the 1.75Gyr-old (Anthony-Twarog et al. 2009) cluster NGC 3680 (solid circles are detections; solid inverted triangles are upper limits) taken from Anthony-Twarog et al. (2009); and the 650 Myr-old Hyades cluster data (open stars are detections, crosses are upper limits) from Balachandran (1995).